Inferring the Subduction Rate and Period over the North Atlantic

JOHN C. MARSHALL,* A. J. GEORGE NURSER,** AND RICHARD G. WILLIAMS*

*Center for Meteorology and Physical Oceanography, Massachusetts Institute of Technology, Cambridge, Massachusetts
**James Rennell Centre for Ocean Circulation, Chilworth Research Centre, Southampton, United Kingdom

(Manuscript received 22 August 1991, in final form 22 June 1992)

ABSTRACT

The annual rate at which mixed-layer fluid is transferred into the permanent thermocline—that is, the annual subduction rate S_{ann} and the effective subduction period $\mathcal{T}_{eff}$—is inferred from climatological data in the North Atlantic. From its kinematic definition, S_{ann} is obtained by summing the vertical velocity at the base of the winter mixed layer with the lateral induction of fluid through the sloping base of the winter mixed layer. Geostrophic velocity fields, computed from the Levitus climatology assuming a level of no motion at 2.5 km, are used; the vertical velocity at the base of the mixed layer is deduced from observed surface Ekman pumping velocities and linear vorticity balance. A plausible pattern of S_{ann} is obtained with subduction rates over the subtropical gyre approaching 100 m/yr—twice the maximum rate of Ekman pumping.

The subduction period $\mathcal{T}_{eff}$ is found by viewing subduction as a transformation process converting mixed-layer fluid into stratified thermocline fluid. The effective period is that period of time during the shallowing of the mixed layer in which sufficient buoyancy is delivered to permit irreversible transfer of fluid into the main thermocline at the rate S_{ann}. Typically $\mathcal{T}_{eff}$ is found to be 1 to 2 months over the major part of the subtropical gyre, rising to 4 months in the tropics.

Finally, the heat budget of a column of fluid, extending from the surface down to the base of the seasonal thermocline is discussed, following it over an annual cycle. We are able to relate the buoyancy delivered to the mixed layer during the subduction period to the annual-mean buoyancy forcing through the sea surface plus the warming due to the convergence of Ekman heat fluxes. The relative importance of surface fluxes (heat and freshwater) and Ekman fluxes in supplying buoyancy to support subduction is examined using the climatological observations of Isemer and Hasse, Schmitt et al., and Levitus. The pumping down of fluid from the warm summer Ekman layer into the thermocline makes a crucial contribution and, over the subtropical gyre, is the dominant term in the thermodynamics of subduction.

1. Introduction

Traditionally Ekman pumping has been viewed as setting the rate at which surface waters are transferred down into the thermocline. However, although fluid is pumped down from the shallow, surface Ekman layer into the mixed layer beneath, it is flow through the spatially and temporally varying base of the mixed layer that actually ventilates the thermocline, as indicated schematically in Fig. 1. Recent tracer studies by Sarmiento (1983) and Jenkins (1987) suggest that the ventilation rate in the North Atlantic is two to three times greater than can be accounted for by Ekman pumping alone; lateral induction of fluid across the sloping base of the mixed layer must also make an important contribution (Woods 1985).

The properties of the main thermocline are controlled by the annual subduction rate since it is this flux that ventilates the *permanent* thermocline. The ventilation mechanism however is intimately related to, and crucially controlled by, the *seasonal cycle* of the mixed layer. Under the action of mechanical and buoyancy forcing the mixed layer seasonally shallows and deepens. However, it is only fluid leaving the mixed layer when it is deep during winter and spring that irreversibly enters the permanent thermocline; fluid subducted from the summer mixed layer is generally re-entrained as the mixed layer deepens the following winter—Stommel's (1979) "mixed-layer demon." This biases (Iselin 1939) the T–S properties of the main thermocline toward those of the deep winter mixed layers.

In the present contribution we attempt to diagnose the annual rate at which fluid passes between the mixed layer and the main (permanent) thermocline S_{ann} from climatological data over the North Atlantic. In section 2, a "kinematic" method is used to calculate S_{ann} by evaluating the yearly volume flux across the fixed Eulerian surface defined by the base of the mixed layer at the end of winter. We employ the Ekman pumping

Corresponding author address: Dr. John C. Marshall, Dept. of Earth, Atmospheric and Planetary Science, Massachusetts Institute of Technology, Center for Meteorology and Physical Oceanography, Building 54, Rm 1526, Cambridge, MA 02139.

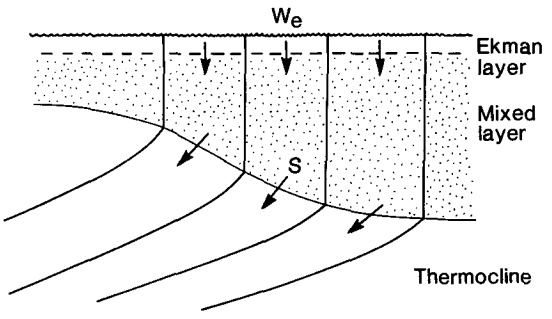

FIG. 1. A schematic diagram showing isopycnals in the thermocline outcropping into a vertically homogeneous mixed layer driven by buoyancy fluxes and Ekman pumping at its surface. Quasi-horizontal flow in the mixed layer slides to and from the thermocline through the sloping base of the mixed layer. The mass flux per unit surface area through the mixed-layer base is S; it is the field of S that ventilates the thermocline.

field of Isemer and Hasse (1987) and the March mixed-layer depth and the lateral flow field derived from the Levitus (1982) climatological hydrographic dataset.

In section 3, we discuss the time period over which this "irreversible" subduction occurs by considering the transfer of mass from a mixed layer undergoing a seasonal cycle. We deduce the "effective subduction period" $\mathcal{T}_{\text{eff}}$, making use of the relation between the instantaneous S and the net buoyancy flux (the surface flux less the buoyancy taken up into the Ekman drift) into the mixed layer obtained in Nurser and Marshall (1991, hereafter NM).

In section 4, we discuss how the buoyancy delivered to the mixed layer during the effective subduction period $\mathcal{B}_{\text{sub}}$ depends on the surface fluxes and the seasonal cycle of the mixed layer. We focus on the buoyancy budget of a column of mixed-layer fluid, following it through an annual cycle (Federiuk and Price 1985; Woods 1985—henceforth FP and Woods). The annual subduction is associated with the shallowing and lightening of the mixed layer over the subduction period. This buoyancy input is simply the annual-mean net flux $\mathcal{B}_{\text{net}}$ less the net buoyancy flux outside the subduction period. We show that this latter flux, which we call $\mathcal{B}_{\text{pump}}$, exactly compensates the pumping down of warm, light surface waters from the summer mixed layer into the seasonal thermocline. In section 5, we estimate the contributions the net surface fluxes and the Ekman pumping make in supplying the necessary buoyancy for subduction using climatological observations and our understanding of the seasonal cycle of the mixed layer.

Due to uncertainties in the climatological observations, particularly the surface fluxes, our estimates are subject to substantial error (simple error estimates are carried out). Only a rather blurred view of the S_{ann} and $\mathcal{T}_{\text{eff}}$ fields is obtained; however, despite these uncertainties, plausible patterns of rates and periods appear and an unambiguous picture emerges.

2. A kinematic estimate of subduction

a. *Definitions of subduction rate*

The instantaneous subduction rate S has been precisely defined as the downward velocity of a parcel of fluid (following the horizontal motion of the parcel) *relative to the base of the mixed layer*—see Cushman-Roisin (1987), NM, and Fig. 2:

$$S = -\frac{\partial h}{\partial t} - \mathbf{u}_b \cdot \nabla h - w_b, \qquad (1)$$

where h is the thickness of the mixed layer, $\mathbf{u}_b$ is the horizontal velocity of the particle at the base of the mixed layer, w_b is its vertical velocity, and t is time. In the presence of any discontinuity, we take $\mathbf{u}_b$ and w_b to be the velocities on the *thermocline* side of the mixed-layer base.

The quantity S is the volume per unit horizontal area per unit time at which thermocline water is created from mixed-layer water; it is the volume flux *across* the moving mixed-layer base. It comprises the temporal mixed-layer term $\partial h/\partial t$, a term representing lateral induction of fluid through the sloping mixed-layer $\mathbf{u}_b \cdot \nabla h$, and the vertical velocity w_b at the base of the mixed layer.

This definition of $S(t)$ does not necessarily involve any physical transfer of fluid between the mixed layer and the permanent thermocline. For example, consider an idealized ocean at rest into which a mixed layer deepens and shallows with the seasonal cycle; see Fig. 3a. In this case, S reduces to

$$S(t) = -\frac{\partial h}{\partial t}.$$

Particles of fluid, although not themselves moving, find themselves either in the mixed layer or the seasonal thermocline merely because of the cycling up and down of the mixed layer. In this limit, there is no net transfer of fluid into the permanent thermocline beneath.

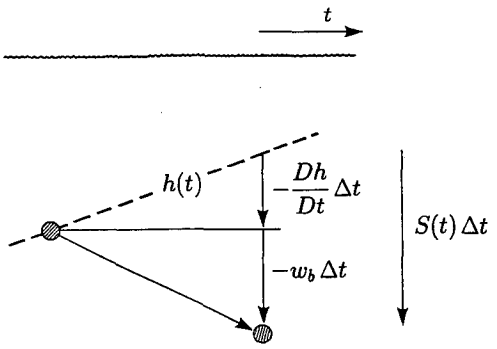

FIG. 2. A schematic diagram showing a particle being subducted from the time-varying base of the mixed layer into the thermocline. The vertical distance between the particle and the mixed layer, $S(t)\Delta t$, is the sum of the vertical displacement of the particle, $-w_b\Delta t$, and the shallowing of the mixed layer following the particle, $-(Dh/Dt)\Delta t$.

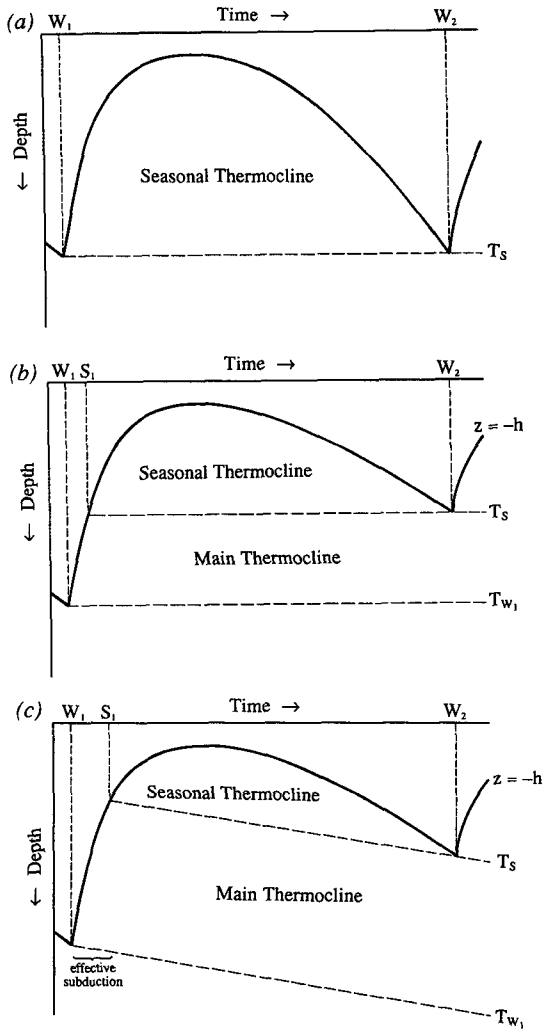

FIG. 3. A schematic mixed-layer cycle in a Lagrangian frame, in which the water column experiences (a) no surface heating or Ekman pumping, (b) only surface heating, (c) only Ekman pumping. The mixed-layer depth (full line) and subducted isotherms (dashed lines) are shown. Fluid is subducted into the permanent thermocline during the effective subduction period between the end of winter W_1 and a later time S_1, which is defined as when the mixed layer has the same temperature T_s as at the end of the second winter W_2. Outside this period, any fluid subducted into the seasonal thermocline is reentrained during the following winter as the mixed layer deepens.

In reality, the seasonal cycle of warming and cooling leads to a deep winter mixed layer, particularly over the subpolar gyre and the northern flank of the subtropical gyre, where it may be hundreds of meters thick (Fig. 4a). The layer shallows in spring and summer to a nearly uniform thickness of typically 30 m. Thus the instantaneous S defined in (1) is dominated over most of the subtropical and the entire subpolar gyre by the temporal change in the mixed-layer depth, which typically shallows by 100 m/mo in spring and deepens by 50 m/mo in autumn and winter. But, over the course of a year, the temporal term must again vanish identically if there is no systematic long-term change in mixed-layer properties. In contrast, the vertical velocity and lateral induction terms, although an order of magnitude smaller (typically reaching values of 50 m yr^{-1}), result in a systematic transfer of fluid particles between the mixed layer and the permanent thermocline. It is this *annual subduction rate across the base of the winter mixed layer* that is the focus of attention in our diagnostic study.

b. *Diagnosing the annual subduction from hydrographic data*

Only fluid subducted from the mixed layer during the effective subduction period, late winter to early spring, penetrates into the main thermocline. Outside

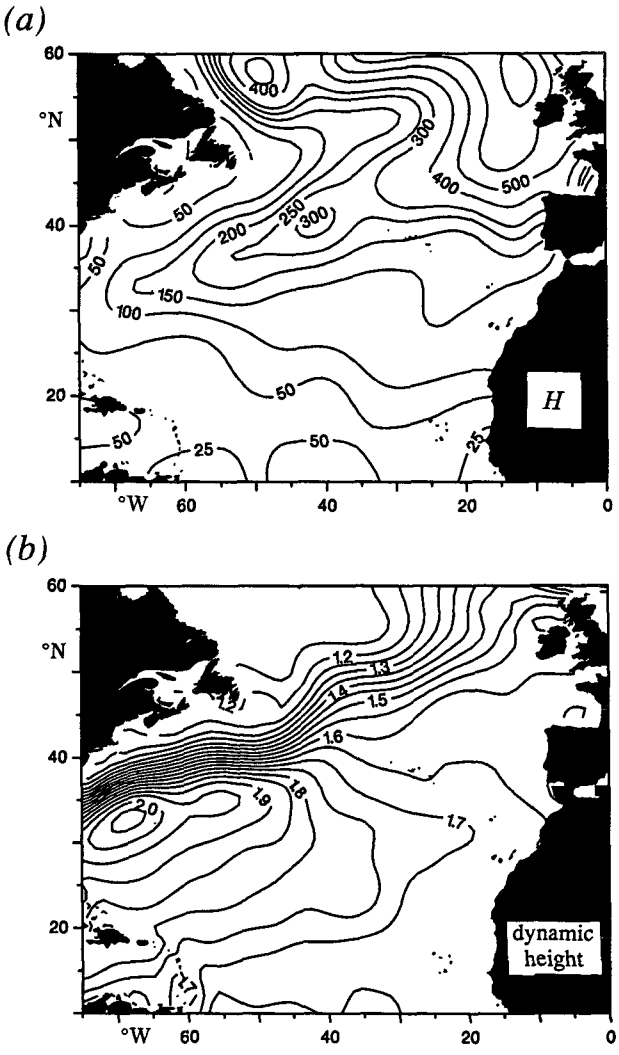

FIG. 4. (a) March mixed-layer depth H (m) from the Levitus (1982) climatology (smoothed to remove fine scales), (b) dynamic height field (m) at 250 m relative to 2500 m derived by integrating the thermal wind equations with the Levitus (1982) climatology.

this period, fluid is temporarily subducted from the shallow summer mixed layer into the seasonal thermocline and is eventually reentrained by the deepening winter mixed layer. All the fluid within the seasonal thermocline and above the winter mixed-layer base, $z = -H$, can thus be considered to have been in recent contact with the atmosphere. The annual subduction S_{ann} into the permanent thermocline is identified with the annual volume flux across this interface $z = -H$ (assuming that the temporal term is identically zero with no interannual variability)[1]:

$$S_{ann} = -\bar{w}_H - \bar{\mathbf{u}}_H \cdot \nabla H. \quad (2)$$

Here the overbar denotes an annual mean and the subscript H denotes the velocity is at the depth H.

The vertical velocity at $z = -H$ may be related to the Ekman pumping using linear vorticity balance, $w_H = w_{Ek} - (\beta/f)\int_{-H}^{0} v dz$, where f is the planetary vorticity and β is its gradient, enabling (2) to be written as

$$S_{ann} = -\bar{w}_{Ek} + \frac{\beta}{f}\int_{-H}^{0} \bar{v} dz - \bar{\mathbf{u}}_H \cdot \nabla H. \quad (3)$$

Thus S_{ann} can be enhanced relative to Ekman pumping by the lateral transfer of fluid out of the winter mixed layer, but is reduced by the meridional transport within the mixed layer.

In our kinematic method S_{ann} is computed from (3) over the North Atlantic using:

(i) The March mixed-layer depth H from the Levitus hydrography (Fig. 4a), defined as the depth at which σ_θ differs by 0.125 from the surface σ_θ.

(ii) The velocity at the base of the winter mixed layer $\mathbf{u}_H$ obtained by integrating the thermal wind equations from a level of no motion chosen to be at 2500 m or (if it is shallower) the seafloor. Levitus winter climatology is used above 1500 m and the annual climatology below 1500 m. The resulting dynamic height field at 250 m is shown in Fig. 4b.

(iii) The annual-mean Ekman vertical velocity from the Isemer and Hasse climatology (Fig. 5a).

The March mixed-layer depth, Fig. 4a, shows a generally poleward deepening reaching down to depths of 500 m or more in the northeast Atlantic. A deep tongue $\geq$ 200 m sweeps southwestward into the subtropical gyre. On the southern flank of the subtropical gyre the mixed layer shallows to less than 50 m at 10°N. The dynamic height, Fig. 4b, clearly reveals the seaward extension of the Gulf Stream carrying fluid to supply the gyres, with anticyclonic and cyclonic flows in the subtropical and subpolar gyre, respectively. There is evidence of a Gulf Stream recirculation, but the major part of the flow sweeps southward and northward at 45°W to supply the gyre interiors.

The vertical velocity at the base of the winter mixed layer is generally smaller in magnitude than the Ekman pumping (Fig. 5b). However, there is a substantial lateral flux of fluid into the main thermocline (Fig. 5c), which usually dominates over the vertical flux.

The resulting S_{ann} field (Fig. 5d) typically reaches 50–100 m yr^{-1} in the subtropical gyre and is enhanced over the local Ekman pumping of typically 25–50 m yr^{-1}.

The surface buoyancy loss along the Gulf Stream deepens the mixed layer along its track and results in large entrainment rates of up to 300 m yr^{-1} due to the lateral transfer of fluid from the thermocline into the mixed layer (Fig. 5c,d). On the southern and western flanks of the Gulf Stream recirculation, the mixed layer shoals leading to a band of high subduction rates of 100 m yr^{-1}. In the subpolar gyre, the entrainment rate reaches 100 to 300 m yr^{-1} and is dominated by the horizontal advection of fluid into the winter mixed layer. This is significantly larger than the local Ekman suction of 50 m yr^{-1}.

Our climatological estimate of S_{ann} is subject to substantial error; assuming the errors in w_H and $\mathbf{u}_H \cdot \nabla H$ are 40% of their absolute values, then the error in S_{ann} is typically $\pm$15 m yr^{-1} in the interior of the gyre or $\sim$30% of the absolute value. While S_{ann} depends on the dynamic height and mixed-layer depth fields, the zero line in the S_{ann} field appears to roughly track the zero Ekman pumping line separating the gyres. The estimate of S_{ann} in the interior of the subtropical gyre is in accord with estimates of 80 $\pm$ 10 m yr^{-1} by Jenkins (1987) using tritium-age observations at the beta-triangle site (centered at 27.5°N, 33.5°W) and the 60–80 m yr^{-1} found in a steady thermocline model of the subtropical gyre with a winter mixed layer by Williams (1991).

Our estimates of S_{ann} cannot be directly compared with the water-mass formation rates deduced by Speer and Tziperman (1992). They estimate the rate at which water masses are formed in a particular density range at the sea surface integrated across the basin. This flux need not be transferred into the permanent thermocline but may instead pass into the mixed layer and seasonal thermocline. Indeed, water mass formation rates and subduction rates may locally even have the opposite sign; for instance, Speer and Tziperman show that there is substantial water mass formation at the sea surface over the subpolar gyre, whereas S_{ann} is generally negative there with entrainment into the mixed layer from the main thermocline.

The properties carried by the flux S_{ann} are thought to be a highly biased mean of the annual cycle because of the nature of the mixed-layer cycle. In the next section, we diagnose the period over which irreversible transfer of properties into the thermocline occurs.

[1] Alternatively, from a Lagrangian perspective, in which a column of mixed-layer fluid is followed (see section 4 and Fig. 3b,c), S_{ann} is given by the Lagrangian change in mixed-layer depth over the year added to the vertical velocity at the base of the mixed layer.

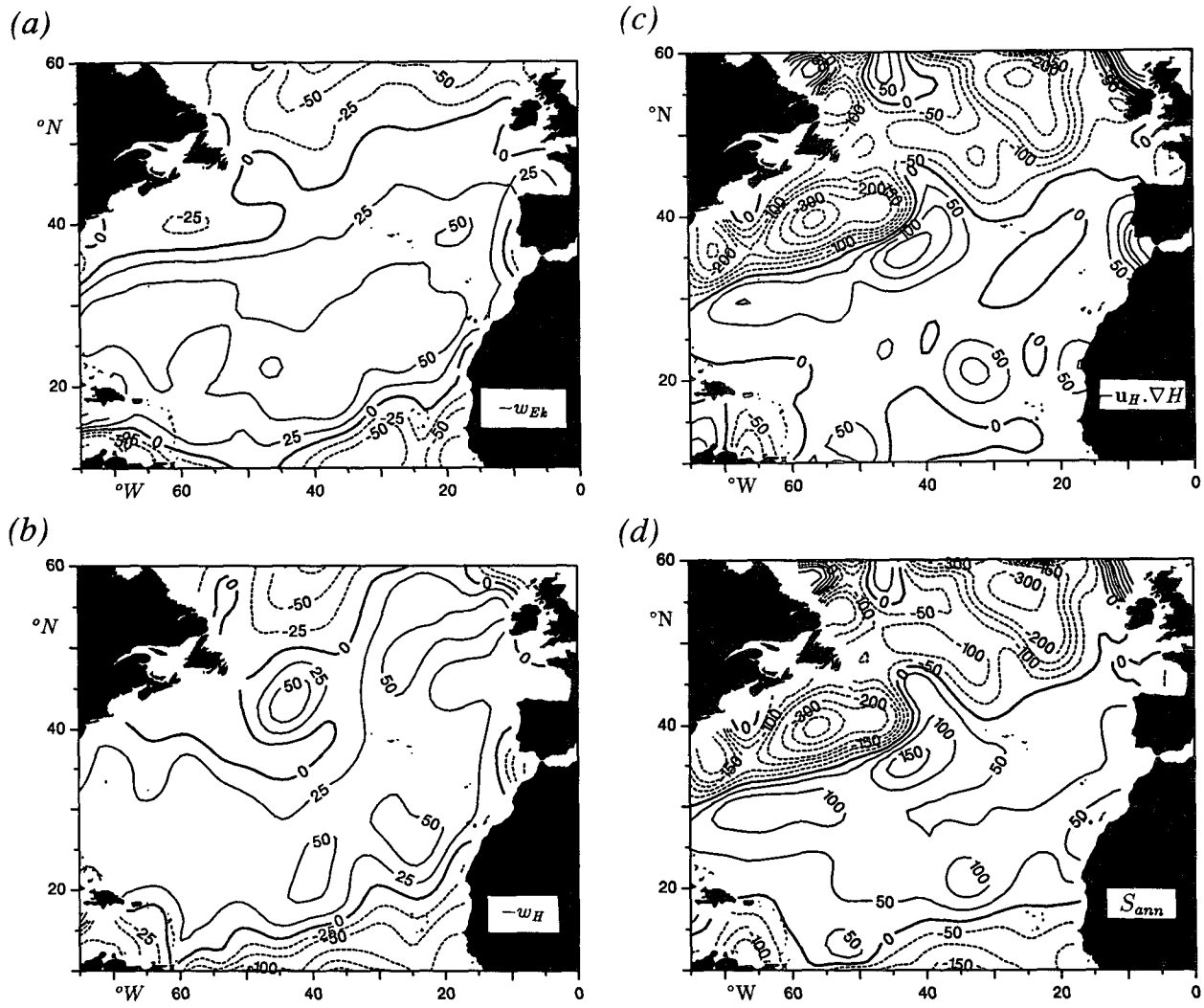

FIG. 5. (a) Annual-mean Ekman pumping, $-w_{Ek}$ (m yr^{-1}) from the Isemer and Hasse (1987) climatology (contours every 25 m yr^{-1}); (b) annual vertical velocity, $-w_H$ (m yr^{-1}) into the main thermocline (contours every 25 m yr^{-1}); (c) annual lateral flux, $-\mathbf{u}_H \cdot \nabla H$, into the main thermocline (contours every 50 m yr^{-1}); (d) annual subduction rate S_{ann} (m yr^{-1}) into the main thermocline (contours every 50 m yr^{-1}).

3. The subduction period

We now attempt to diagnose the subduction period $\mathcal{T}_{eff}$ making use of the thermodynamic budget of the mixed layer. To explain our method we link the kinetic definition of S to the thermodynamic forcing of the mixed layer.

a. Buoyancy forcing and the instantaneous subduction rate

The instantaneous subduction rate can, as shown in NM, be related to the buoyancy forcing of the mixed layer by making use of the thermodynamic equation for the mixed layer.

As long as the density and potential vorticity of a parcel of fluid are conserved once it is subducted into the thermocline and density is continuous at the base of the mixed layer (as in Fig. 1), the large-scale potential vorticity

$$Q_b \equiv -\frac{f}{\bar{\rho}} \frac{\partial \rho}{\partial z}\bigg|_{z=-h}$$

of the fluid being subducted into the thermocline may be related to the mixed-layer thickness h and density ρ_m through the purely kinematic relation (see Cushman-Roisin 1987; Williams 1989)

$$Q_b = -\frac{f D_b \rho_m / Dt}{\bar{\rho} S}. \tag{4}$$

Here $D_b/Dt = (\partial/\partial t) + \mathbf{u}_b \cdot \nabla$ is the material derivative following the geostrophic flow just below the base of

the mixed layer; when there is no density jump at the base of the mixed layer, $\mathbf{u}_b$ is continuous and equal to the *geostrophic* velocity just above the base of the mixed layer.

By thermal wind, that component of the geostrophic flow within the mixed layer that is *parallel* to $\nabla\rho_m$ is independent of depth. Hence, the material derivative of density following the geostrophic flow, $D_b\rho_m/Dt$, is also uniform throughout the mixed layer, allowing the thermodynamic equation for the mixed layer to be expressed as

$$\frac{D_b\rho_m}{Dt} = -\frac{\mathcal{B}_{\text{net}}}{gh}, \tag{5}$$

where $\mathcal{B}_{\text{net}}$ is defined as the "net" buoyancy flux

$$\mathcal{B}_{\text{net}} = \frac{g\alpha}{C_w}\mathscr{H}_{\text{in}} - g\beta_s\mathscr{S}_{\text{in}} - \mathcal{B}_{\text{Ek}}. \tag{6}$$

This is made up of:

(i) The surface heat flux $\mathscr{H}_{\text{in}}$; here α is the thermal expansion coefficient and C_w the heat capacity of water.

(ii) The surface salt flux $\mathscr{S}_{\text{in}} = \bar{\rho}s_m(E - P)$; here s_m is the mixed-layer salinity, β_s the haline contraction coefficient, and E and P the evaporation and precipitation rates, respectively.

(iii) The buoyancy flux acquired by the Ekman drift

$$\mathcal{B}_{\text{Ek}} = \frac{g}{\bar{\rho}f}\,\mathbf{k}\times\tau\cdot\nabla\rho_m. \tag{7}$$

Here, τ is the wind-stress, g is the gravitational acceleration, and $\mathbf{k}$ the unit vertical vector.

By combining the kinematic relations (1) and (4) with the buoyancy balance of the mixed layer (5), NM showed that S can be related to the net buoyancy flux, the mixed-layer thickness, and the potential vorticity at the base of the mixed layer, thus[2]:

$$S = \frac{f\mathcal{B}_{\text{net}}}{g\bar{\rho}hQ_b} = -\mathcal{B}_{\text{net}}\Big/\left(gh\frac{\partial\rho}{\partial z}\Big|_b\right). \tag{8}$$

The sign of S takes on the sign of the buoyancy flux through the sea surface less the advection by the Ekman drift. Furthermore the magnitude of S depends on $\mathcal{B}_{\text{net}}/hQ_b$, and so is dependent on the strength of buoyancy forcing and, crucially, on the depth and stratification at the base of the mixed layer. A moderate $\mathcal{B}_{\text{net}}$ equivalent to 20 W m^{-2} acting on a mixed layer of $h \sim 100$ m, at whose base the stratification is 3 kg m^{-3}/km (equivalent to $Q_b = 3\times10^{-10}$ m^{-1} s^{-1} if $f = 10^{-4}$ s^{-1}) can drive a substantial flux of $S \sim 100$ m yr^{-1}. Note that S does not depend explicitly on the Ekman pumping field and can even have the opposite sign to w_{Ek}; this is strikingly evident in some of the pedagogical examples given in NM.

The quantities of climatic importance are the annual subduction rate S_{ann} and the interval of time over which the subduction occurs $\mathcal{T}_{\text{eff}}$ because it sets the properties of the permanent thermocline. We wish to diagnose the subduction period by using the subduction relation (8) and our knowledge of the seasonal mixed-layer cycle. However, before we proceed further, the assumptions that underpin the subduction relation (8) should be clearly stated:

(i) Density is continuous at the base of the mixed layer. Without this the kinematic relation (4) is not valid. Furthermore "entrainment fluxes" through the base of the mixed layer become important when there is mixed-layer deepening and should be included as an extra term in the thermodynamic equation (5).

(ii) The thermocline is adiabatic and inviscid.

These are both reasonable assumptions in the midlatitude oceans during the winter to spring period when fluid is subducted into the *permanent* thermocline.

b. *The effective subduction period*

The seasonal cycle of warming and cooling leads to a deep winter mixed layer, particularly over the subpolar gyre and the northern flank of the subtropical gyre (Fig. 4a), which shallows in spring and summer to a nearly uniform thickness. The annual subduction is controlled by this regional variation in the seasonal cycle of the mixed layer; this is illustrated in the idealized models of FP, Woods, Cushman-Roisin (1987), and Woods and Barkmann (1988).

A period of *effective* subduction can be defined when fluid passes irreversibly into the permanent thermocline (Fig. 3b,c); S_{ann} is then given by the integrated subduction through the base of the mixed layer during this period from the end of winter W_1 to the time S_1:

$$S_{\text{ann}} = \frac{1}{\mathcal{T}_{\text{year}}}\int_{W_1}^{S_1} S(t)\,dt. \tag{9}$$

Here, $\mathcal{T}_{\text{year}}$ is one year, and the instantaneous subduction $S(t)$ may be defined by the kinematic relation (1) or during mixed-layer shallowing by the subduction relation (8).

[2] This relation (8) can be generalized to allow buoyancy forcing on both sides of the mixed-layer base. If Q is discontinuous across the base of the mixed layer but density is continuous, it can be shown that the volume flux across the base of the mixed layer [see Eq. (32), Marshall and Nurser 1992]

$$S = \mathbf{u}\cdot\mathbf{n} = \frac{[B\omega\cdot\mathbf{n}]}{g\rho[Q]},$$

where $\mathbf{u}$ is the velocity and $\mathbf{n}$ is the normal vector to the surface. Here, σ is the potential density, ω is the absolute vorticity, $B = -gD\sigma/Dt$ is the buoyancy forcing, and $Q = -\rho^{-1}\omega\cdot\nabla\sigma$ is the full Ertel potential vorticity. Square brackets [ ] denote the change in the enclosed quantity across the surface. We recover (8) if we assume that buoyancy forcing is confined within the mixed layer and vanishes in the thermocline, and $Q_b \gg Q_{\text{mix}}$ (the potential vorticity in the mixed layer). The approximate expression (8) is used here in order to permit diagnostic progress to be made with the climatological data.

Property distributions in the main thermocline suggest that the effective period is in the spring (Iselin 1939) when the mixed layer begins to warm and rapidly shallow from its deep winter maximum. Outside this effective period, fluid is subducted from the mixed layer into the seasonal thermocline and is subsequently reentrained into the deepening mixed layer during the following winter (Fig. 3b,c).

c. *Diagnosing the subduction period from climatological data*

We now deduce the subduction period by combining our kinematic estimate of S_{ann} in (9) with an estimate of the instantaneous $S(t)$ using the buoyancy forcing relation (8):

$$S_{\text{ann}} = \frac{1}{\mathcal{T}_{\text{year}}\bar{\rho}g}\int_{W_1}^{S_1}\frac{\mathcal{B}_{\text{net}}}{hQ_b}\,dt, \qquad (10a)$$

where the net buoyancy flux is given by

$$\mathcal{B}_{\text{net}} = \frac{g\alpha}{C_w}\mathcal{H}_{\text{in}} - g\beta_s\mathcal{S}_{\text{in}} - \mathcal{B}_{\text{Ek}}. \qquad (10b)$$

The instantaneous subduction is estimated using observed monthly values of the net buoyancy flux $\mathcal{B}_{\text{net}}$, mixed-layer depth h, and potential vorticity at the base of the mixed-layer Q_b. The net buoyancy flux is calculated, as described in more detail in section 5a, from the surface heat flux of Isemer and Hasse (1987), the water flux of Schmitt et al. (1989), and the Ekman flux derived from the wind stress of Isemer and Hasse and the surface density of Levitus (1982). The mixed-layer depth and stratification are calculated from the monthly density fields derived from the Levitus monthly temperature and seasonal salinity fields.

The integration of $S(t)$ over the subduction period in (10) should be made in a Lagrangian frame, in which one follows a column of fluid as it is swept around the gyre. Here, however, for convenience, we choose to integrate $S(t)$ using Eulerian values of $\mathcal{B}_{\text{net}}$, h, and Q_b. This is a reasonable assumption if the subduction period lasts only a few months (as is the case over the major part of the subtropical gyre).

The effective subduction into the main thermocline starts when the mixed layer first starts shallowing at the onset of buoyancy forcing in the spring. We define this starting time W_1 to be when $\mathcal{B}_{\text{net}}$ changes sign; it ranges from January to February in the subtropics and from March to April in the subtropical gyre. In entrainment regions, W_1 is the time when the effective entrainment from the main thermocline into the mixed layer/seasonal boundary layer finally ceases; it ranges from March to April over the subpolar gyre and until May over the Gulf Stream.

The effective subduction period $\mathcal{T}_{\text{eff}}$ as deduced from (10), is shown in Fig. 6. It endures for 1 to 2 months over most of the subtropical gyre. It is somewhat longer,

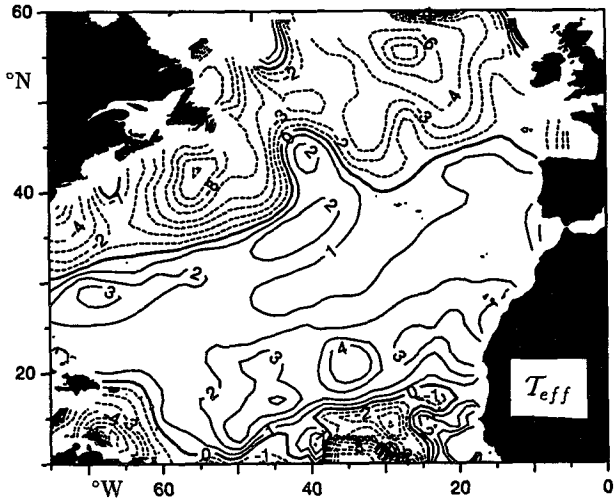

FIG. 6. Subduction period (months) inferred from the kinematic estimate of the subduction rate and the seasonal of buoyancy forcing; positive values indicate subduction into the main thermocline occurs after the end of winter, whereas negative values indicate entrainment from the main thermocline occurs prior to the end of winter.

3 or 4 months, in the subtropics where the mixed layer is shallower and its depth cycle is less pronounced, and so fluid is pumped directly from the summer mixed layer into the main thermocline. However, in those regions where the subduction period extends into the summer, our estimate should be regarded as a lower bound, since we do not incorporate possible fluxes of heat out of the base of the mixed layer by either entrainment fluxes or the penetration of solar radiation.

In the subpolar gyre, fluid is irreversibly entrained from the main thermocline into the mixed layer/seasonal boundary layer over an effective period of 2 to 4 months before the end of winter (denoted by negative values in Fig. 6).

The effective subduction period is a direct measure of Stommel's "mixed-layer demon" (1979) idea that fluid being subducted into the main thermocline carries with it the end of winter mixed-layer characteristics. We expect the main thermocline to have property distributions that match the mixed-layer fields during this effective period, rather than the annual-mean mixed-layer properties. The data indeed suggests that properties of the main thermocline in the subtropical gyre are highly biased toward the end of winter mixed-layer properties (Iselin 1939); for instance, in the interior of the subtropical gyre, the potential vorticity of the main thermocline closely matches the winter mixed-layer boundary conditions, rather than the summer conditions (Williams 1991).

An interesting aspect of the subduction relation (10) is the modulating role of the stratification at the base of the seasonal mixed layer; examples are given in NM. Figure 7 shows the Q_b field in March (a) and June (b). In March, when subduction starts, we see very weak

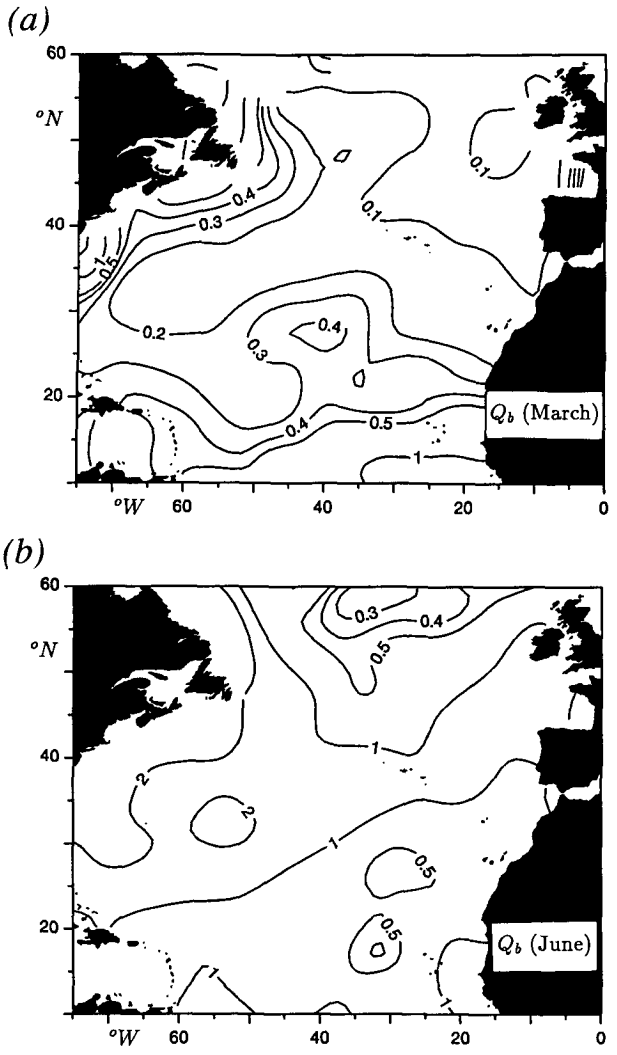

FIG. 7. The potential vorticity at the base of the mixed layer Q_b (10^{-9} m^{-1} s^{-1}) during (a) March and (b) June computed from the Levitus climatology.

stratification at the base of the deep, winter mixed layer. The spacing of isopycnals at the top of the thermocline is large and fluid can readily flow into the mixed layer—instantaneous subduction rates are very large. In June, however, the mixed layer is shallow and the stratification at its base is an order of magnitude larger than in March. This larger stratification closes the "throat" of the thermocline making the transfer of fluid between the mixed layer and the thermocline much more difficult.

d. *Diagnosing the heat flux during the subduction period*

The annual subduction is associated with a buoyancy flux $\mathcal{B}_{\text{sub}}$, which is given by the net buoyancy flux occurring over the effective subduction period:

$$\mathcal{B}_{\text{sub}} = \frac{1}{\mathcal{T}_{\text{year}}} \int_{W_1}^{S_1} \mathcal{B}_{\text{net}}(t)\,dt. \qquad (11)$$

It can be diagnosed from the monthly values of the net buoyancy flux (10b) occurring over the effective subduction period. For clarity, we discuss the buoyancy forcing in terms of an equivalent heat flux by defining

$$\mathcal{H}^* = C_w \mathcal{B}/(\bar{\alpha} g),$$

where starred variables are always *pseudo* heat fluxes and $\bar{\alpha}$ is evaluated using the annual-mean mixed-layer temperature.

The equivalent heat flux $\mathcal{H}^*_{\text{sub}}$ driving the subduction over the few months of the effective subduction period is typically 5 to 10 W m^{-2} of warming over the subtropical gyre and -25 to -50 W m^{-2} of cooling over the subpolar gyre (Fig. 8). The entrainment into the deepening mixed layer along the Gulf Stream requires -50 to -100 W m^{-2} of cooling, and the subduction on the southern flank of the Stream requires a heating of 10 W m^{-2}.

Observations show that the product of h and Q_b vary only by a factor of 2 over the subduction period, whereas they separately vary by almost an order of magnitude (Fig. 7). To estimate the error in $\mathcal{H}^*_{\text{sub}}$, we approximate the integral (11) by combining with (10):

$$\mathcal{H}^*_{\text{sub}} = \frac{1}{\mathcal{T}_{\text{year}}} \int_{W_1}^{S_1} \mathcal{H}^*_{\text{net}}\,dt \sim \frac{\bar{\rho} C_w}{\bar{\alpha} f} h Q_b S_{\text{ann}}.$$

Ascribing an error of 40% to hQ_b and using our previous estimate of a 30% error in S_{ann} suggests an error in $\mathcal{H}^*_{\text{sub}}$ of ~50% or typically ±5 to ±10 W m^{-2}. This is somewhat smaller than the errors in the monthly fluxes, which are themselves at least ±20 W m^{-2}. Such uncertainties in $\mathcal{H}^*_{\text{net}}$ primarily affect our estimate of the subduction period, $\mathcal{T}_{\text{eff}}$, which is probably in error by

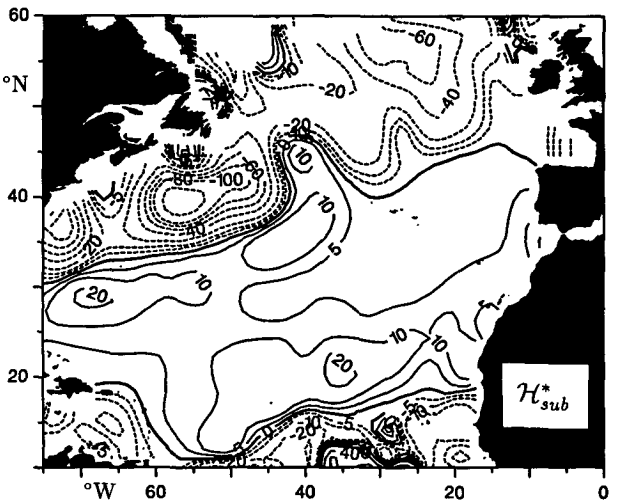

FIG. 8. The heat flux $\mathcal{H}^*_{\text{sub}}$ (W m^{-2}) into the ocean that drives the subduction of fluid into the main thermocline; positive values are associated with subduction and negative values with entrainment.

as much as ±1 month. However, the integrated heat flux over this period, $\mathscr{H}^*_{sub}$, is relatively insensitive to such errors and is instead contaminated by somewhat smaller errors in our kinematic estimate of S_{ann}.

4. The thermodynamics of subduction

We now discuss how the heat flux $\mathscr{H}^*_{sub}$ is made available to the subduction process through the interplay of the atmospheric forcing and the seasonal cycle of the mixed layer. For simplicity, we couch our discussion in terms of the heat balance, but in the subsequent diagnostic calculations we consider the analogous buoyancy balance and take into account salinity changes from surface freshwater fluxes.

Let us follow a vertical column of mixed-layer fluid that is assumed to move barotropically (typical annual displacements are shown in Fig. 9); the advection of heat by the baroclinic shear is found to be relatively unimportant and is neglected here (see Appendix). Consider first the annual march, from winter (W_1) through spring (S_1) to the following winter (W_2), of a mixed layer. Assume that winter on winter, the mixed layer warms and shallows (as in Fig. 3b,c); the increase in heat content of the mixed layer and the seasonal thermocline is achieved by the surface heat fluxes and/or the convergence of Ekman heat fluxes. Let S_1 be the time in the cycle when the mixed layer has the same temperature as its coldest value the following winter:

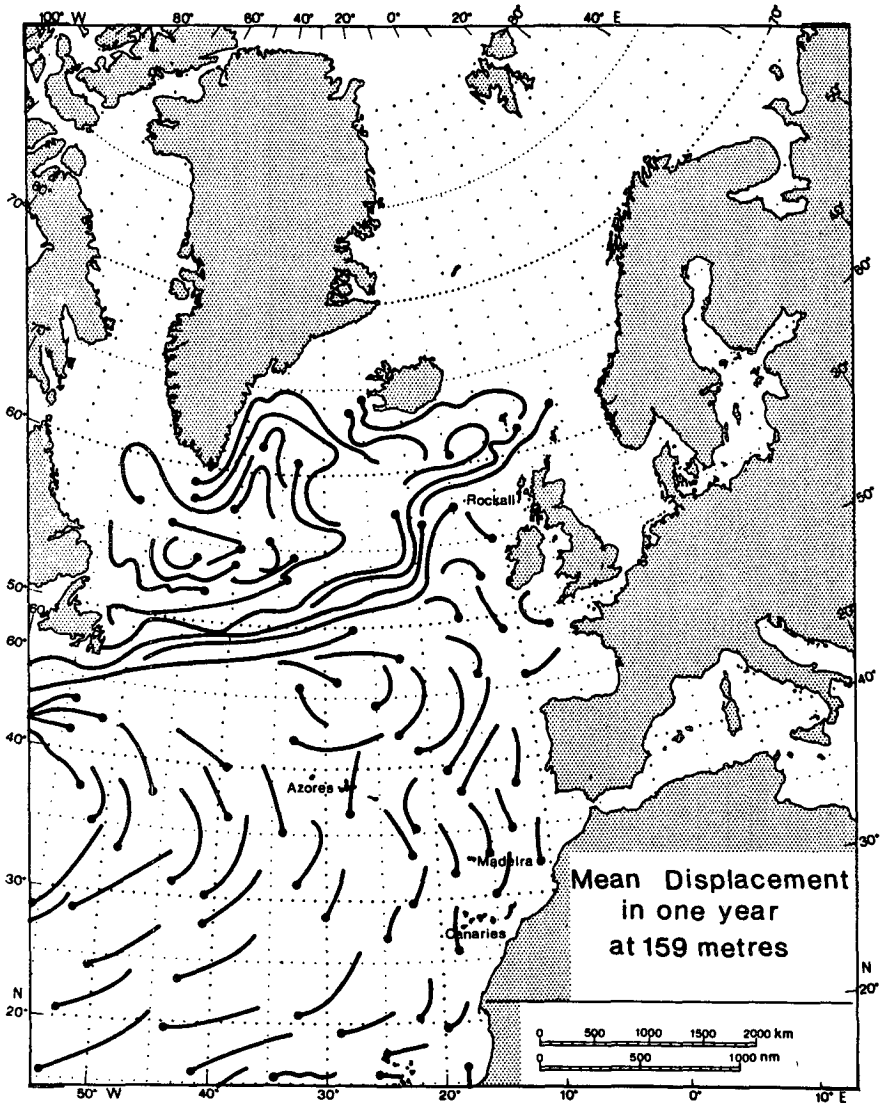

FIG. 9. Mean displacement of fluid parcels in one year at a depth of 159 m from the model of Sarmiento and Bryan (1982) (displayed in Woods 1987).

$$T_{S_1} = T_{W_2} > T_{W_1}.$$

Let us further assume that at both S_1 and W_1 temperature at the base of the mixed layer is continuous with that in the thermocline. Then this temperature $T_{S_1} = T_{W_2}$ (which we shall write as T_s) defines the base of the seasonal thermocline: warmer water ($T > T_s$) is only temporarily subducted into the seasonal thermocline, whereas during the "effective" subduction period, cooler water ($T_m < T_s$) passes from the mixed layer into the permanent thermocline.

The net heat input into the mixed layer over the effective subduction period,

$$\mathscr{H}_{\text{sub}} T_{\text{year}} = \int_{W_1}^{S_1} \mathscr{H}_{\text{net}} dt, \tag{12a}$$

may be expressed in terms of the annual-mean heat input minus the heat input outside the subduction period,

$$\int_{W_1}^{S_1} \mathscr{H}_{\text{net}} dt = \int_{W_1}^{W_2} \mathscr{H}_{\text{net}} dt - \int_{S_1}^{W_2} \mathscr{H}_{\text{net}} dt. \tag{12b}$$

We consider two idealized cases; first a mixed-layer cycle in the absence of Ekman pumping but with an annual-mean heating and, second, with Ekman pumping but no annual-mean heating.

a. Annual-mean heating and no Ekman pumping

Let us assume that there is a net heating applied to the mixed layer over the annual cycle $\bar{\mathscr{H}}_{\text{net}} > 0$ so that the mixed layer warms and shallows from W_1 to W_2 (Fig. 3b) leaving fluid behind and hence, resulting in subduction into the main thermocline; FP and Woods discuss this case.

Since the mixed layer has the same T and h and hence the same heat content at the times S_1 and W_2, then there is no heat input outside the subduction period. Consequently, the heat input supplied to the mixed layer over the subduction period, W_1 to S_1, is the same as that supplied from the annual-mean net heating and so (12) reduces to

$$\mathscr{H}_{\text{sub}} = \bar{\mathscr{H}}_{\text{net}}.$$

b. Ekman pumping and no annual-mean heating

Now let us consider how the heat balance is modified in the presence of Ekman pumping. Fluid particles now have a vertical motion and so, after subducting from the shallowing mixed layer in the spring, they slide down along sloping isopycnals into the thermocline (Fig. 3c). The convergence of the horizontal Ekman heat fluxes leads to a pumping down of warm waters from the Ekman layer into the thermocline. The crucial effect of this heat gain of the fluid column is that the mixed layer at W_2 becomes shallower and warmer than in the preceding winter W_1. It is this shallowing that results in subduction, a point emphasized by FP.

The heat input during the subduction period now depends on the annual-mean heat input *minus* the heat lost outside the subduction period (12b). So how do we compute this heat loss outside the subduction period and what is its physical significance?

Assuming that all the diabatic heat fluxes (including entrainment fluxes) are confined within the mixed layer and the seasonal thermocline, ($T > T_s$), then the heat balance following the water column is given by

$$\bar{\rho} C_w \int_{z_s(t)}^{0} \left(\frac{\partial T}{\partial t} + w \frac{\partial T}{\partial z} \right) dz = \mathscr{H}_{\text{net}}, \tag{13}$$

where $z_s(t)$ is the depth of the isotherm T_s.

Let us assume for simplicity that $\partial w/\partial z = 0$ within the mixed layer and the seasonal thermocline, that is, that the column is vertically nondivergent, with $w(z) \equiv w_{\text{Ek}}$, then

$$\bar{\rho} C_w \left\{ \int_{z_s(t)}^{0} \frac{\partial T}{\partial t} dz + w_{\text{Ek}} (T_m - T_s) \right\} = \mathscr{H}_{\text{net}},$$

which (noting that $\partial z_s/\partial t = w_{\text{Ek}}$) may then be written as

$$\bar{\rho} C_w \frac{\partial}{\partial t} \int_{z_s(t)}^{0} T dz = \mathscr{H}_{\text{net}} - \bar{\rho} C_w w_{\text{Ek}} T_m, \tag{14}$$

where T_m is the mixed-layer temperature. Equation (14) is a statement of the heat content of the fluid column, from the surface down to the depth of the isotherm T_s. Its physical context is perhaps best revealed by expanding $\mathscr{H}_{\text{net}} = \mathscr{H}_{\text{in}} - \mathscr{H}_{\text{Ek}}$; on the right-hand side of (14) thus becomes

$$\mathscr{H}_{\text{in}} - \bar{\rho} C_w (\mathbf{U}_{\text{Ek}} \cdot \nabla T_m + w_{\text{Ek}} T_m).$$

Here, $\mathscr{H}_{\text{Ek}} = \bar{\rho} C_w \mathbf{U}_{\text{Ek}} \cdot \nabla T_m$ is the heat flux balancing the Ekman drift, where $\mathbf{U}_{\text{Ek}} = -(\mathbf{k} \times \tau)/(\bar{\rho} f)$ is the horizontal Ekman flux per unit horizontal length, and $\bar{\rho} C_w w_{\text{Ek}} T_m$ is the heat flux due to the Ekman pumping of fluid from the mixed layer into the seasonal thermocline. The heat content can be changed by (i) heat fluxes through the sea surface, (ii) Ekman drift, and (iii) Ekman pumping. Since $w_{\text{Ek}} = \nabla \cdot \mathbf{U}_{\text{Ek}}$, the latter two terms can be combined, thus

$$\mathbf{U}_{\text{Ek}} \cdot \nabla T_m + w_{\text{Ek}} T_m = \nabla \cdot (\mathbf{U}_{\text{Ek}} T_m)$$

and represent simply the divergence of the horizontal Ekman heat fluxes. In our discussion, however, we prefer to distinguish between Ekman drift and pumping contributions because they represent distinct (although related) processes, and, furthermore, only $\mathscr{H}_{\text{Ek}}$ appears in the subduction relation (8).

Returning now to (14), we integrate with respect to time outside the subduction period, S_1 to W_2, and noting that $T_{S_1} = T_{W_2} = T_s$ at these limits of integration gives

$$(z_s(S_1) - z_s(W_2))\bar{\rho} C_w T_s = \int_{S_1}^{W_2} \mathscr{H}_{\text{net}} dt - \int_{S_1}^{W_2} \bar{\rho} C_w w_{\text{Ek}} T_m dt.$$

Furthermore, since $z_s(S_1) - z_s(W_2) = \int_{S_1}^{W_2} w_{\text{Ek}} dt$,

$$\int_{S_1}^{W_2} \mathscr{H}_{\text{net}} dt = \int_{S_1}^{W_2} \bar{\rho} C_w w_{\text{Ek}} (T_m - T_s) dt. \quad (15a)$$

We see that heat must be lost outside the subduction period if there is Ekman pumping $w_{\text{Ek}} < 0$; this loss cancels out the excess heat content of the fluid, with $T > T_s$, pumped down from the warm summer Ekman layer into the seasonal thermocline. We write this heat flux as an annual-average flux $\mathscr{H}_{\text{pump}}$ defined by

$$\mathscr{H}_{\text{pump}} \mathcal{T}_{\text{year}} = \int_{S_1}^{W_2} \mathscr{H}_{\text{net}} dt. \quad (15b)$$

The effect of this pumping of warm water downward is that the mixed layer at W_2 is warmer (and shallower) than the preceding winter W_1. It is this warming that results in subduction. This crucial point can be made explicit as follows.

During the period S_1 to W_2, the Ekman pumping–induced warming is exactly compensated [see (15)] by a net heat loss, which is just sufficient to ensure that the mixed layer cools to the temperature T_s by W_2. Thus, since in this thought experiment there is no net annual-mean heating,

$$\int_{W_1}^{S_1} \mathscr{H}_{\text{net}} dt + \int_{S_1}^{W_2} \mathscr{H}_{\text{net}} dt = 0,$$

and so in this case (12) reduces to

$$\mathscr{H}_{\text{sub}} = -\mathscr{H}_{\text{pump}}.$$

Thus, the warming of the mixed layer that is driving subduction during the effective subduction period exactly balances the heat loss occurring outside the effective subduction period: $-\mathscr{H}_{\text{pump}}$ may be thought of as driving the subduction in the special case when $\bar{\mathscr{H}}_{\text{net}} = 0$.

In the general case where there is an annual net heat flux and Ekman pumping, the heat flux driving subduction is given by

$$\mathscr{H}_{\text{sub}} = \bar{\mathscr{H}}_{\text{net}} - \mathscr{H}_{\text{pump}}. \quad (16)$$

Using typical values of $w_{\text{Ek}} = 10^{-6}$ m s^{-1} ($\sim$30 m yr^{-1}) and a summer maximum of $T_m - T_s = 5$°C suggests that the heat flux $-\mathscr{H}_{\text{pump}}$ reaches 20 W m^{-2} of warming. This is comparable to the annual-mean net heat flux into the ocean $\bar{\mathscr{H}}_{\text{net}}$.

5. Diagnosing the contributions to the heat flux during subduction

We wish to determine the relative contributions of $\bar{\mathscr{H}}^*_{\text{net}}$ and $\mathscr{H}^*_{\text{pump}}$ to $\mathscr{H}^*_{\text{sub}}$ from climatological data:

$$\mathscr{H}^*_{\text{sub}} = \bar{\mathscr{H}}^*_{\text{net}} - \mathscr{H}^*_{\text{pump}}.$$

Again, to avoid confusion, the * is used to represent *pseudo* heat fluxes (rescaled buoyancy fluxes). The preceding relation is appropriate for a Lagrangian frame, but for diagnostic purposes we adopt an Eulerian frame, a reasonable approximation provided that the spatial scale over which the buoyancy fluxes vary is much greater than the distance that fluid columns move over a year. Over the interior of the subtropical gyre, fluid parcels are displaced by typically $\sim$500 km (Fig. 9), but in the vicinity of the Gulf Stream, displacements are considerably greater, and fluxes vary over comparable distances. Thus, errors in an Eulerian calculation may be expected to be large over the Gulf Stream and near the zero line of net annual buoyancy gain where there are large gradients.

We now discuss the various terms contributing to the thermal forcing of the mixed layer, and then examine the separate contributions to the heat balance (16).

a. Terms contributing to the annual net heat flux

1) THE ANNUAL SURFACE HEAT FLUX

The surface heat flux results from the inbalance between solar, net infrared, latent, and sensible heat fluxes over the year. The seasonal cycle in the surface heat flux induces the mixed-layer cycle of deepening and shallowing.

According to the Isemer and Hasse climatology[3], there is a small annual heat input into the subtropical gyre (a few W m^{-2}) and a cooling of typically -25 to -50 W m^{-2} over the subpolar gyre (Fig. 10a). The signature of the Gulf Stream is particularly apparent as the region of maximum heat loss of typically -200 W m^{-2}. The errors in this climatology are substantial, and at least ± 20 W m^{-2}. They ultimately limit our attempt to separate $\mathscr{H}^*_{\text{sub}}$ into component parts.

The solar heat flux penetrating below the winter mixed layer reaches 1 W m^{-2} in the subtropical gyre or a maximum of 10 W m^{-2} in the tropics where there is a shallow mixed layer, and is thus neglected here.

2) THE ANNUAL SURFACE WATER FLUX

The surface buoyancy flux into the ocean depends upon the surface water flux, as well as the surface heat

[3] Isemer and Hasse estimate that the annual surface heat loss over the North Atlantic south of 65°N is -17 W m^{-2}, whereas it is only -4 W m^{-2} in the original Bunker (1976) fields. They argue that the Bunker (1976) climatology implies a zonally averaged, meridional, oceanic heat transport at 25°N of only 0.8 PW (1 PW = 10^{15}W), whereas a larger value of 1.2 PW is suggested by Hall and Bryden (1982) and Wunsch (1984) using independent observations. Isemer and Hasse therefore modify the original Bunker (1976) climatology by adjusting cloud amount, wind speed, transfer coefficients, and air–sea temperature difference, so as to imply a meridional heat transport of 1 PW; however, note that the Bunker (1988) climatology with smaller net infrared fluxes is also consistent with 1 PW at 25°N.

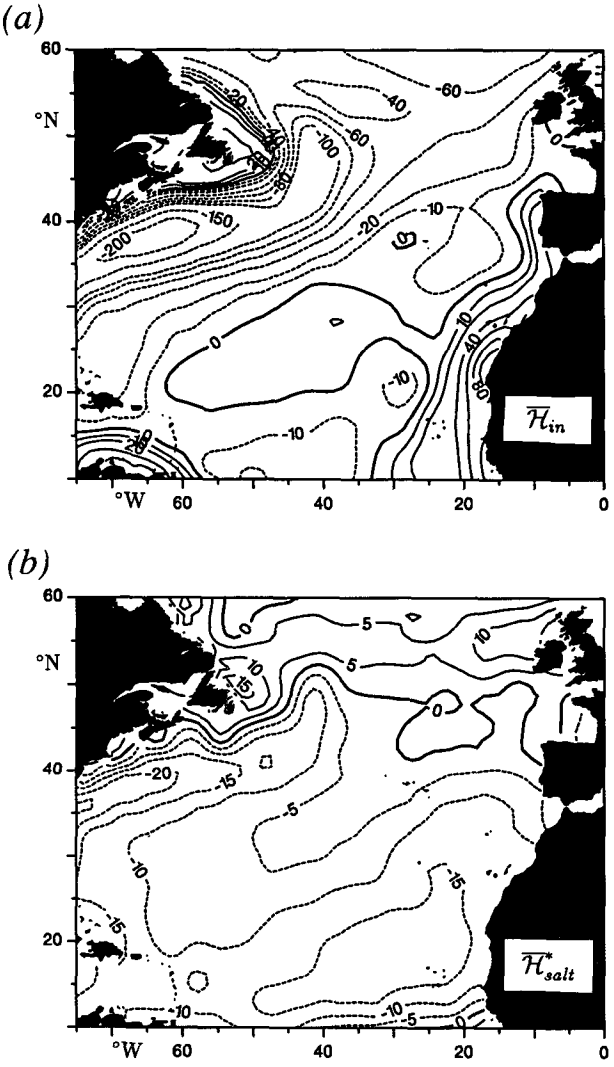

FIG. 10. (a) The annual-mean surface heat flux $\bar{\mathcal{H}}_{in}$ (W m^{-2}) from the Isemer and Hasse (1987) climatology; positive values indicate a heat flux into the ocean. (b) The annual-mean equivalent heat flux $\bar{\mathcal{H}}^*_{salt}$ (W m^{-2}) associated with freshwater fluxes derived from the Schmitt et al. (1989) climatology.

flux. We compute a pseudo heat flux (see Fig. 10b) from the surface salt flux of Schmitt et al. (1989)

$$\mathcal{H}^*_{salt} = -C_w\beta_s\mathcal{S}_{in}/\bar{\alpha},$$

where the salt flux is calculated from the evaporation of Bunker (1976) and the precipitation of Dorman and Bourke (1981). Over most of the subtropical gyre, evaporation exceeds precipitation giving a net surface water loss of ~0.75 m yr^{-1}, which leads to a buoyancy loss equivalent to −5 to −10 W m^{-2} of cooling (Fig. 10b). North of 45°N and south of 10°N, precipitation exceeds evaporation and there is a corresponding buoyancy input. Comparing the fields of $\bar{\mathcal{H}}_{in}$ and $\bar{\mathcal{H}}^*_{salt}$ shows that they are comparable to each other over the southern and eastern parts of the subtropical gyre (Fig. 10a,b).

3) THE ANNUAL EKMAN-DRIFT HEAT FLUX

The Ekman heat flux is that flux absorbed by the cross-isopycnal Ekman drift (7):

$$\mathcal{H}^*_{Ek} = \frac{C_w}{\bar{\alpha}\rho f}\,\mathbf{k}\times\tau\cdot\nabla\rho_m.$$

The annual-mean Ekman flux is calculated from the annual mean of the monthly values using the wind stress from Isemer and Hasse and the mixed-layer density from Levitus.

The wind stress drives an annual-mean Ekman drift into warmer regions north of 30°N, which requires an effective heating of 10 W m^{-2} (Fig. 11). Over the southern part of the subtropical gyre, the northward Ekman drift requires an effective cooling, which becomes particularly strong south of 20°N where the horizonal density gradient is large and the Coriolis parameter is small. Over the tropics, Behringer and Stommel (1981) also show a northward Ekman drift and, in their annual heat budget, they deduce that it must be almost entirely compensated by a surface buoyancy loss.

b. The heat flux driving subduction

We now compute $\mathcal{H}^*_{sub}$ directly from the separate contributions of $\mathcal{H}^*_{net}$ and $\mathcal{H}^*_{pump}$, and compare with our kinematic estimate shown in Fig. 8.

1) THE ANNUAL-MEAN NET HEAT FLUX

The equivalent annual-mean net heat flux is calculated from the annual-mean contributions of surface heat and water fluxes, minus the Ekman flux

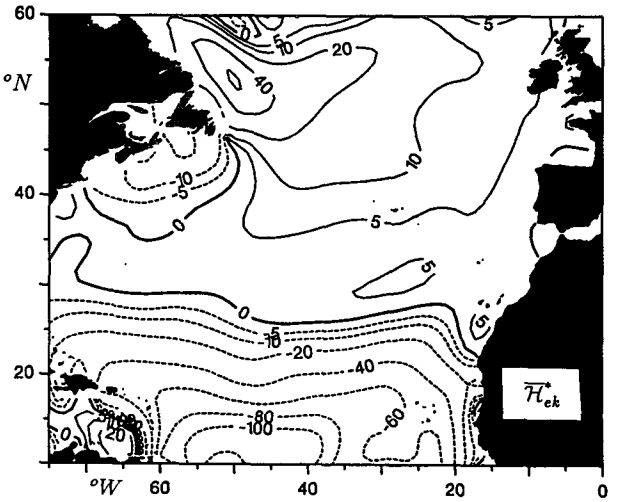

FIG. 11. The annual-mean heat flux $\bar{\mathcal{H}}^*_{Ek} = (C_w/\overline{\alpha\rho}f)\overline{\mathbf{k}\times\tau\cdot\nabla\rho_m}$, taken up into the Ekman drift (in W m^{-2}).

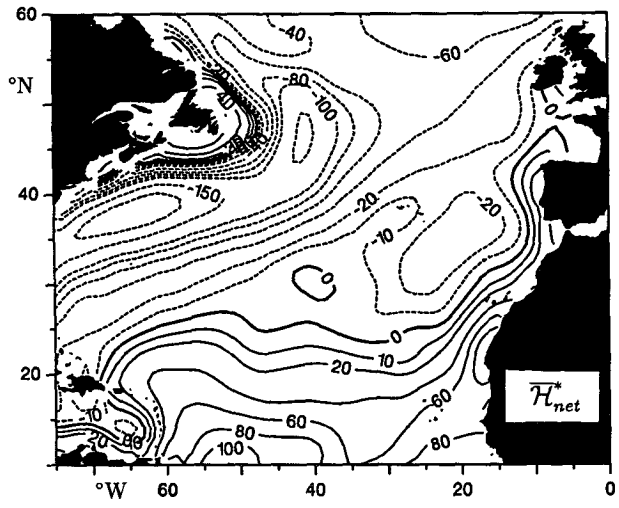

FIG. 12. The annual-mean net heat flux, $\bar{\mathcal{H}}^*_{net} = \bar{\mathcal{H}}^*_{in} + \bar{\mathcal{H}}^*_{salt} - \bar{\mathcal{H}}^*_{Ek}$ (in W m^{-2}).

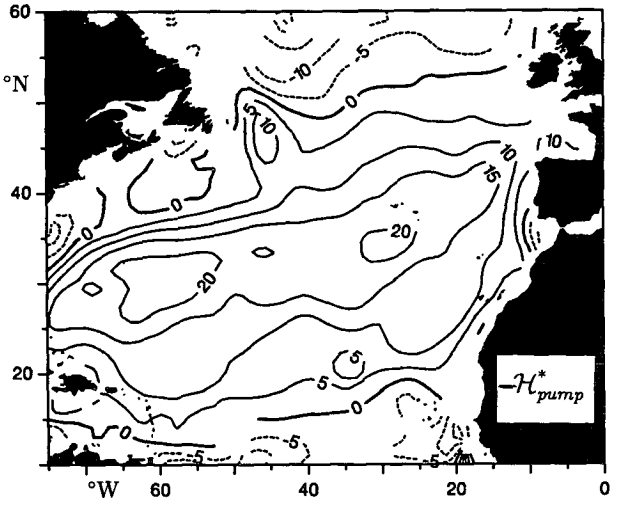

FIG. 13. The heat flux $\mathcal{H}^*_{pump} = (C_w/\bar{\alpha}\mathcal{T}_{year}) \int_{S_1}^{W_2} w_{Ek}[\rho_S - \rho_m(t)]dt$ (in W m^{-2}).

$$\bar{\mathcal{H}}^*_{net} = \bar{\mathcal{H}}^*_{in} + \bar{\mathcal{H}}^*_{salt} - \bar{\mathcal{H}}^*_{Ek},$$

and is plotted in Fig. 12. There is a net heat loss over most of the subtropical gyre and all of the subpolar gyre. We note, however, that the subduction field derived from the independent kinematic relation requires a small heat *input* over the subtropical gyre (see $\mathcal{H}^*_{sub}$ in Fig. 8).

Over the interior of the subtropical gyre, the mismatch between $\mathcal{H}^*_{sub}$ and $\bar{\mathcal{H}}^*_{net}$ is typically 20 W m^{-2} (see Fig. 15a where the difference field is plotted). Due to the large errors in the fluxes, particularly $\bar{\mathcal{H}}^*_{net}$, this difference could be attributed to large systematic errors; however, we believe that this difference has a physical significance and is, at least in part, a signature of $\mathcal{H}^*_{pump}$. We now compute $\mathcal{H}^*_{pump}$ and the difference field, $\bar{\mathcal{H}}^*_{net} - \mathcal{H}^*_{pump}$, which ought to balance $\mathcal{H}^*_{sub}$ [see (16)].

2) THE NET HEAT FLUX OUTSIDE THE SUBDUCTION PERIOD

The net heat flux outside the subduction period (15), balancing the Ekman pumping of buoyant fluid into the seasonal thermocline, is diagnosed here using

$$\mathcal{H}^*_{pump} = \frac{C_w}{\bar{\alpha}\mathcal{T}_{year}} \int_{S_1}^{W_2} w_{Ek}[\rho_S - \rho_m(t)]dt$$

and can be computed using the subduction period, the monthly values of w_{Ek} and mixed-layer density ρ_m and ρ_S, the mixed-layer density at the end of winter, from the Levitus climatology.

We show the heat flux $-\mathcal{H}^*_{pump}$ in Fig. 13. In the subtropical gyre, $-\mathcal{H}^*_{pump}$ reaches 20 W m^{-2} of warming, as is required to support subduction. Even though there is a large seasonal density cycle here, $\mathcal{H}^*_{pump}$ is smaller in magnitude in the subtropics because the subduction period lengthens and thus reduces the period of time $\mathcal{H}_{pump}$ has to act. In the subpolar gyre, $-\mathcal{H}^*_{pump}$ only gives a heat flux of -5 W m^{-2} due to the smaller seasonal density cycle at higher latitudes. We see that the sign and magnitude of $\mathcal{H}^*_{pump}$ is such that it acts to reduce the difference between $\mathcal{H}^*_{sub}$ and $\bar{\mathcal{H}}^*_{net}$.

3) COMPARISON WITH THE HEAT FLUX–DRIVEN SUBDUCTION

We plot $\bar{\mathcal{H}}^*_{net} - \mathcal{H}^*_{pump}$ in Fig. 14, which ought to balance our independent estimate of $\mathcal{H}^*_{sub}$ [see (16)]. Using the Isemer and Hasse climatology, there is a net heat loss $\bar{\mathcal{H}}^*_{net}$ over most of the subtropical gyre and

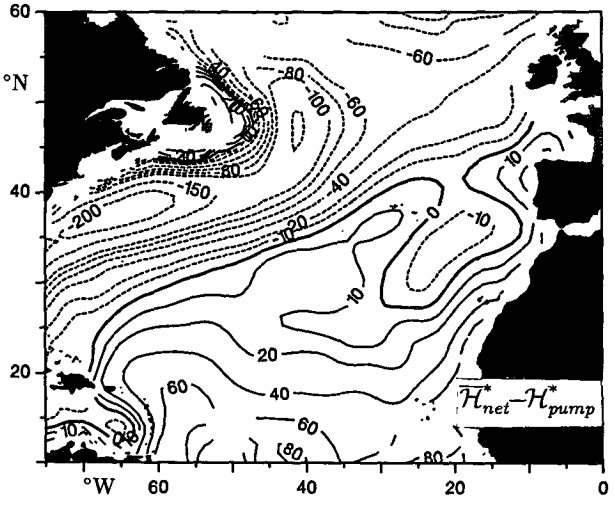

FIG. 14. $\bar{\mathcal{H}}^*_{net} - \mathcal{H}^*_{pump}$, an estimate of $\mathcal{H}^*_{sub}$ (in W m^{-2}).

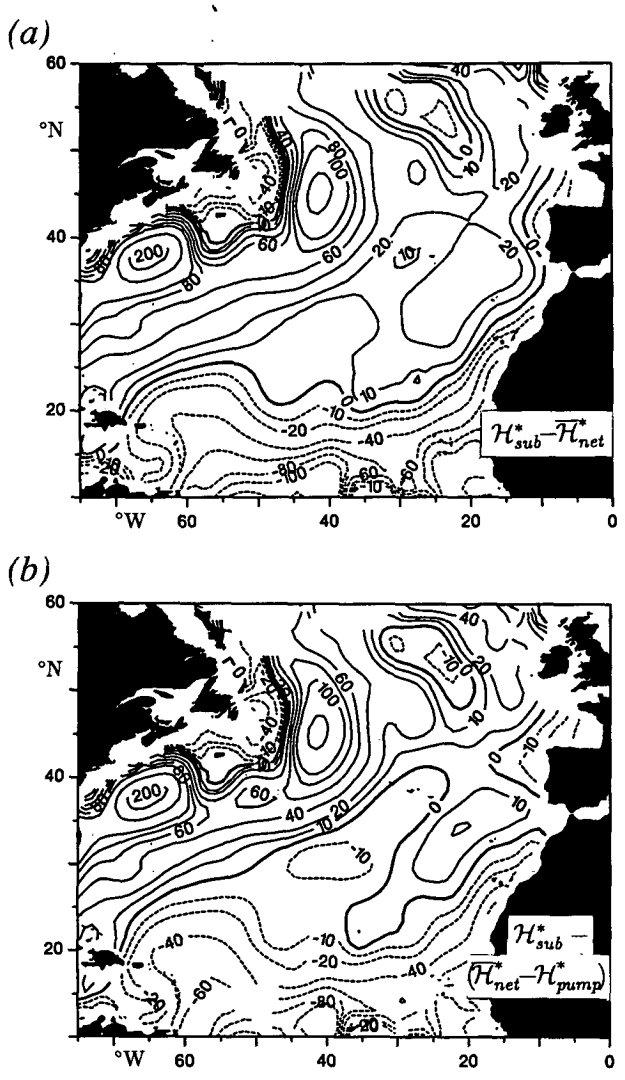

FIG. 15. Difference fields (W m^{-2}): (a) $\mathscr{H}^*_{sub} - \bar{\mathscr{H}}^*_{net}$, (b) $\mathscr{H}^*_{sub} - (\bar{\mathscr{H}}^*_{net} - \mathscr{H}^*_{pump})$.

the entire subpolar gyre. However, the contribution from $\mathscr{H}^*_{pump}$, leads to $\bar{\mathscr{H}}^*_{net} - \mathscr{H}^*_{pump}$ being positive over most of the subtropical gyre (Fig. 14) with the zero contour displaced northward by up to 15°, compared with the annual-mean net heat flux (Fig. 12). Figure 14 is consistent with subduction, rather than entrainment, over most of the subtropical gyre.

Over the interior of the subtropical gyre, the difference between the independent estimates of $\mathscr{H}^*_{sub}$, in Fig. 8 from the kinematic calculation and that deduced in Fig. 14 from the surface fluxes and the seasonal cycle, $\bar{\mathscr{H}}^*_{net} - \mathscr{H}^*_{pump}$, is now typically ±10 W m^{-2} (Fig. 15b). These differences are smaller in magnitude and, moreover, horizontal scale than those implied if $\mathscr{H}^*_{pump}$ is ignored. We suggest that the remaining differences over the interior of the subtropical gyre are principally due to regional errors in $\bar{\mathscr{H}}_{net}$ of at least ±20 W m^{-2}, with the errors in $\mathscr{H}^*_{sub}$ and $\mathscr{H}^*_{pump}$ being somewhat smaller.

Over the Gulf Stream, much larger discrepancies are found reaching 75 W m^{-2}; $\bar{\mathscr{H}}^*_{net} - \mathscr{H}^*_{pump}$ implies a large heat loss suggesting much more entrainment than is found in the kinematic calculation (Fig. 14b). This may be a consequence of using climatologies that smear out the Gulf Stream, but may also be due to the surface heat loss being partly compensated by geostrophic eddy heat flux divergences which cannot be neglected here; the vigorous eddy field tends to flux warm fluid into the Gulf Stream region and this term is not included in our heat budget for the mixed layer.

It is interesting to note that the reduced rate of subduction in the northeastern part of the subtropical gyre (Fig. 5d) appears to be consistent with a tongue of low buoyancy fluxes extending southwestward from the zero line west of Portugal (Fig. 14). This is probably due to the strong, dry trade winds decreasing the buoyancy input into the ocean (see Fig. 10a,b) and so reducing the subduction of fluid here.

6. Conclusions

The annual subduction rate over the North Atlantic has been diagnosed from climatological data. The terms in the kinematic definition of S have been evaluated from hydrographic data by computing the flux across the surface defined by the base of the winter mixed layer assuming a level of no motion at 2.5 km and linear vorticity balance. The effective subduction period has been obtained from hydrography and climatological fluxes of buoyancy exploiting our understanding of the thermodynamics of the seasonal mixed-layer cycle and its role in controlling the annual subduction rate.

The subduction rates reach 100 m yr^{-1} over the subtropical gyre, typically twice the Ekman pumping. The enhancement over and above that due to Ekman pumping is due to the lateral induction of fluid through the sloping base of the mixed layer. In the subpolar gyre, entrainment rates reach 300 m yr^{-1} or more over wide areas and are associated with the advection of fluid by the cyclonic gyre into the mixed-layer deepening to the north.

The effective subduction period is short, only ~2 months, over most of the subtropical gyre, lengthening to 4 months in the tropics.

A definitive discussion and illustration of the thermodynamic process associated with subduction is made difficult by the large uncertainty in the climatology of the surface heat and momentum fluxes. However, despite these errors, we are able to obtain a consistent picture in which the pumping down of fluid from the warm summer Ekman layer into the seasonal thermocline leads to the warming and shallowing of the mixed layer driving the subduction process.

Finally, our kinematic diagnostics of S_{ann} combined with an understanding of the seasonal cycle of the mixed layer could provide strong additional constraints on the surface heat and momentum fluxes, which are

presently notoriously difficult to estimate with any certainty.

Acknowledgments. JCM was supported in part by the National Science Foundation of the U.S., AJGN by the Natural Environment Research Council of the U.K. under the UKWOCE special topic, and RGW by the University Corporation of Atmospheric Research of the U.S., under the NOAA Program in Climate and Global Change.

APPENDIX

Baroclinic Advection

The discussion in section 4 assumes that we are following the barotropic motion of a fluid column. However, by thermal wind, there must be baroclinic shear in the top few hundred meters, so fluid columns tilt sideways as they move. If we still wish to follow a vertical column, it can no longer be a *material* column, and we must include baroclinic advection terms in the heat budget. We find, however, that these terms are small and generally negligible.

Let us first define a little more precisely the velocity of our vertical column. Over the period W_1 to S_1 (the effective subduction period) we move with the geostrophic velocity $\mathbf{u}_b$ just below the mixed layer. Over the 'summer' period S_1 to W_2 we track the fluid parcel with temperature T_s, that is subducted at a time S_1 and just reentrained at W_2. We suppose this particle moves with velocity $\mathbf{u}_s$.

Over the effective subduction period, W_1 to S_1, the following baroclinic advection term apparently appears in the heat budget of the mixed layer:

$$\bar{\rho} C_w \int_{-h}^{0} \mathbf{u}' \cdot \nabla T_m dz,$$

where $\mathbf{u}' = \mathbf{u}_g - \mathbf{u}_b$, is the deviation of the horizontal velocity from the column velocity. However, since ∇T (and hence, by thermal wind, $\partial \mathbf{u}'/\partial z$) does not vary with depth within the mixed layer, then

$$\mathbf{u}' = \mathbf{k} \times \nabla T_m (z + h) \perp \nabla T_m.$$

and this term vanishes; this was used to derive Eq. (5).

However, outside the subduction period, this baroclinic advection term does contribute to the heat balance because we now integrate over the seasonal thermocline within which ∇T may change direction. However, so long as ∇T does not change too rapidly, this term remains small.

Let us estimate the magnitude of the baroclinic advection term, compared with the heat fluxes, $\mathscr{H}_{\text{net}}$ and $\mathscr{H}_{\text{pump}}$, which may typically reach 20 W m^{-2}. At any instant

$$\mathscr{H}_{\text{adv}} = \bar{\rho} C_w \int_{z_s}^{-h} \mathbf{u}' \cdot \nabla T dz,$$

where now $\mathbf{u}' = \mathbf{u} - \mathbf{u}_s$. Assuming that the thickness of the seasonal thermocline, $z_s - h$, reaches 100 m, $\nabla T \sim 10^{-6}$ °C m^{-1}, and the component of $\mathbf{u}'$ *parallel* to $\nabla T \sim 1$ cm s^{-1}, then the instantaneous $\mathscr{H}_{\text{adv}} \sim 4$ W m^{-2}. Therefore, we can neglect $\mathscr{H}_{\text{adv}}$ as it is much smaller than the annual-mean values of $\mathscr{H}_{\text{net}}$ and $\mathscr{H}_{\text{pump}}$.

REFERENCES

Behringer, D. W., and H. Stommel, 1981: Annual heat gain of the tropical Atlantic computed from subsurface ocean data. *J. Phys. Oceanogr.*, **11**, 1393–1398.

Bunker, A. F., 1976: Computations of surface energy flux and annual air-sea interaction cycles of the North Atlantic. *Mon. Wea. Rev.*, **104**, 1122–1140.

——, 1988: Surface energy fluxes of the South Atlantic Ocean. *Mon. Wea. Rev.*, **116**, 809–823.

Cushman-Roisin, B., 1987: *Dynamics of the Oceanic Surface Mixed-Layer.* Hawaii Inst. of Geophysics Special Publication, P. Muller and D. Henderson, Eds.

Dorman, C. E., and R. H. Bourke, 1981: Precipitation over the Atlantic Ocean, 30°S to 70°N. *Mon. Wea. Rev.*, **109**, 554–563.

Federiuk, J. M., and J. F. Price, 1985: Mechanisms of oceanic subduction. [Unpublished manuscript.]

Hall, M. M., and H. L. Bryden, 1982: Direct estimates and mechanisms of ocean heat transport. *Deep-Sea Res.*, **29**, 339–359.

Iselin, C. O'D., 1939: The influence of vertical and lateral turbulence on the characteristics of waters at mid-depths. *Trans. Amer. Geophys. Union*, **20**, 414–417.

Isemer, H. J., and L. Hasse, 1987: *The Bunker Climate Atlas of the North Atlantic Ocean, Vol. 2.* Springer-Verlag, 252 pp.

Jenkins, W. J., 1987: ^{3}H and ^{3}He in the beta triangle: Observations of gyre ventilation and oxygen utilization rates. *J. Phys. Oceanogr.*, **17**, 763–783.

Levitus, S., 1982: *Climatological Atlas of the World Ocean.* NOAA Prof. Paper No. 13, Washington D.C., 173 pp.

Marshall, J. C., and A. J. G. Nurser, 1992: Fluid dynamics of thermocline ventilation. *J. Phys. Oceanogr.*, **22**, 583–595.

Nurser, A. J. G., and J. C. Marshall, 1991: On the relationship between subduction rates and diabatic forcing of the mixed layer. *J. Phys. Oceanogr.*, **21**, 1793–1802.

Sarmiento, J. L., 1983: A tritium box model of the North Atlantic thermocline. *J. Phys. Oceanogr.*, **13**, 1269–1274.

——, and K. Bryan, 1982: An ocean transport model for the North Atlantic. *J. Geophys. Res.*, **87**, 394–408.

Schmitt, R. W., P. S. Bogden, and C. E. Dorman, 1989: Evaporation minus precipitation and density fluxes for the North Atlantic. *J. Phys. Oceanogr.*, **19**, 1208–1221.

Speer, K., and E. Tziperman, 1992: Rates of water mass formation in the North Atlantic Ocean. *J. Phys. Oceanogr.*, **22**, 93–104.

Stommel, H., 1979: Determination of watermass properties of water pumped down from the Ekman layer to the geostrophic flow below. *Proc. Nat. Acad. Sci. U.S.A.*, **76**, 3051–3055.

Williams, R. G., 1989: The influence of air–sea interaction on the ventilated thermocline. *J. Phys. Oceanogr.*, **19**, 1255–1267.

——, 1991: The role of the mixed layer in setting the potential vorticity of the main thermocline. *J. Phys. Oceanogr.*, **21**, 1803–1814.

Woods, J. D., 1985: *Physics of thermocline ventilation. Coupled Atmosphere-Ocean Models.* J. C. J. Nihoul, Ed., Elsevier.

——, 1987: The Warmwatersphere of the Northeast Atlantic-A miscellany. 2nd ed. *Ber. Inst. Meereskd. Univ. Kiel, 128*, 47 pp.

——, and W. Barkmann, 1988: A Lagrangian mixed-layer model of Atlantic 18 degree water formation. *Nature*, **319**, 574–576.

Wunsch, C., 1984: An eclectic model of the North Atlantic circulation. Part I: The meridional flux of heat. *J. Phys. Oceanogr.*, **14**, 1703–1723.